PAPER

NJC
www.rsc.org/njc

Study of *n*-hexane adsorption in MCM-41 mesoporous materials: a scaling effect approach of capillary condensation processes

Philippe Trens,* Nathalie Tanchoux, Daniel Maldonado, Anne Galarneau, Francesco Di Renzo and François Fajula

Laboratoire de Matériaux Catalytiques et Catalyse en Chimie Organique (CNRS/ENSCM UMR 5618), Institut Gerhardt FR 1878, 8 rue de l'Ecole Normale, 34296, Montpellier cedex 5, France. E-mail: ptrens@cit.enscm.fr; Fax: +33 4 67 16 34 70; Tel: +33 4 67 16 34 84

***Received* (in Montpellier, France) 22nd January 2004, Accepted 18th March 2004**
First published as an Advance Article on the web 15th June 2004

The adsorption of hexane on mesoporous MCM-41 materials having different pore sizes has been studied by thermodynamic means. Additional information about their textural properties has been found using the BET model and by tracing comparison plots. Extremely low C_{BET} parameters have been found, confirming the very low affinity of alkanes for siliceous surfaces while comparison plots evidenced true mesoporous materials. The adsorbate-adsorbent interactions have been derived from the isosteric method. A correlation between the heat of condensation and the pore size has been demonstrated and is discussed. The enthalpic contribution of the liquid–gas interface to the overall process has been derived and precisely matches the difference between the enthalpy of condensation in the bulk and the enthalpy condensation in mesopores as large as 10 nm.

Introduction

There is still a need to understand capillary condensation phenomena in small mesopores. This effect is classically described by the Kelvin equation:

$$\ln\left(\frac{p}{p^{\circ}}\right) = -\frac{2\gamma V_{\mathrm{m}}}{RT} \qquad (1)$$

which indicates that the equilibrium pressure p of a spherical particle increases as its radius r decreases, the other parameters of the equation being the saturation pressure p°, the surface tension γ, the molar volume V_{m}, the gas constant R and the temperature T. Eqn. (1) is also valid for the adsorption in porous systems. In this case, a meniscus of condensed phase presents a negative radius and the equilibrium pressure is lower for smaller pores. An important assumption in the Kelvin equation is that the surface tension γ of the condensed phase can be considered as constant over the whole range of pore sizes, or particle sizes, considered.

Several early observations indicated that the Kelvin equation does not provide a precise evaluation of the equilibrium pressure for the phases adsorbed in the smallest mesopores.[1] This phenomenon has been attributed to a dependence of the surface tension on the curvature radius.[2–4] The discovery of micelle-templated ordered silicas with a narrow distribution of mesopore size has made available ideal reference materials for the study of adsorption-desorption mechanisms.[5] Most recent research has been devoted to elucidating the behaviour of adsorbates in the smallest mesopores, in which confinement effects bring about the disappearance of the hysteresis loop of the type IV isotherm.[6] When the adsorption-desorption isotherm does not exhibit a hysteresis loop the pore filling mechanism is still argued.[7] It has been shown that, in such conditions, the heat of condensation of the fluid in the pores of the material is intermediate between the heat of adsorption in a microporous adsorbent and the heat of condensation of the bulk fluid from the vapour phase.[8] For larger mesopores a classical mechanism of capillary condensation can be accepted, implying the activated formation of a meniscus and the corresponding hysteresis in the adsorption-desorption cycle. The purpose of this study is the investigation of the thermodynamics of adsorption in the intermediate range of pore sizes (3–10 nm) in which adsorption-desorption cycles are no longer reversible while a significant effect of confinement can still be expected.

Experimental

Hexane used as an adsorbate was provided by Aldrich (purity >99.9%) and stored over activated 3 Å molecular sieve. The adsorbents used in this work are mesoporous silicas prepared in the presence of either hexadecyltrimethyl ammonium cations (3.1 nm MCM-41),[5,9,10] in some cases accompanied by a swelling agent such as hexadecyldimethylamine (3.8 nm MCM-41),[11] or trimethylbenzene (5.6 nm MCM-41 and 9.9 nm MCM-41).[1,12] All samples were calcined under air flow at 823 K. The most significant textural properties of the adsorbents, as evaluated by nitrogen adsorption at 77 K, are summarized in Table 1. The BET model has been used to determine the specific surface area S_{BET} of each of the materials, while mesopore volumes V_p were measured as the adsorbed amount at the top of the adsorption step of the isotherm.

Mean pore diameters D_p can be estimated by several methods. The classical model built by Barrett, Joyner and Halenda (BJH) for the determination of the pore size distribution through the Kelvin law seriously underestimates the size of small mesopores.[13,14] Better results can be obtained by using a NLDFT approach[15] or from the geometric layout of the periodic pore system itself,[16] while a more classical method, first proposed by Broekhoff and de Boer (BdB), taking into account the curvature of the pore section,[11,17] has proven useful. D_{BdB} in Table 1 have been calculated by applying this method to the adsorption branch of the N_2 isotherms. The Gurvitsch rule of equivalent diameter ($D_p = 4V_p/S_{BET}$) can also be applied to derive average pore sizes, provided pores are cylindrical.[1,14]

Hexane sorption measurements have been performed using a home-built apparatus.[18] Two capacitative pressure gauges (Inficon CR090, temperature compensated at 318 K, 10 torr

DOI: 10.1039/b401094a

Table 1 Specific surface area, mean pore size and mesopore volume of the adsorbents measured by N_2 adsorption at 77 K

	$S_{BET}/m^2\ g^{-1}$	D_p/Å $4V/S$	 BdB	$V_p/cm^3\ g^{-1}$
3.1 nm MCM-41	965	30	31	0.73
3.8 nm MCM-41	1180	38	38	1.11
5.6 nm MCM-41	944	53	56	1.24
9.9 nm MCM-41	854	93	99	1.99

and 1000 torr, provided by Leybold Vacuum) were used to measure equilibrium pressures as well as to derive adsorbed amounts. This set-up has been built in a climatic chamber allowing studies between 250 K and 350 K with a temperature stability better than 0.1 K. Blank experiments performed without any adsorbent have shown that, in the experimental conditions used in this work, side adsorption on the apparatus itself could account for less than 0.5% of the overall adsorption quantities for the adsorption isotherms shown hereafter. The adsorption isotherms have been corrected accordingly from the blank at all temperatures used. The adsorbed isotherms determined with this apparatus are reproducible and one of those shown hereafter (having the same pore diameter as that of ref. 19) perfectly matches the adsorption isotherm of hexane over a 4.0 nm MCM-41 published by Jänchen *et al.*[19]

Results

The general influence of pore size over the adsorption-desorption isotherms is shown in Fig. 1, where the results obtained at 303 K are represented.

All the isotherms belong to type IV in the IUPAC classification, typical of mesoporous solids, and the hysteresis loop tends to vanish in the case of the smaller mesopores. More information can be extracted from the isotherms when they are linearised through the BET equation:

$$\frac{p/p^\circ}{n \times (1 - p/p^\circ)} = \frac{1}{n_m \times C} + \frac{C-1}{n_m \times C} \times p/p^\circ \qquad (2)$$

The Brunauer, Emmett and Teller (BET) model is based on three assumptions: (i) lateral interactions between adsorptive molecules are negligible, (ii) the adsorbent surface is seen as homogeneous by the adsorptive, and (iii) the first adsorbed monolayer interacts with the surface with the same energy E_1 while any other adsorbed monolayers interact with the same energy E_l, E_l being the condensation enthalpy of the adsorptive. In the system we chose, it is clear that these assumptions are fulfilled as: (i) hexane does not exhibit any active function that could interact with the siliceous surface, (ii) intermolecular interactions between hexane molecules are known to be weak,[20] and (iii) it will be shown later that the pore wall–adsorptive interaction is very weak and does not extend further than the first adsorbed monolayer. This system is therefore an ideal one as what we are interested in is the capillary condensation phenomenon, occurring in the core of the pores where the influence of both the nature of the pore walls and their interaction with adsorptive molecules can be neglected.

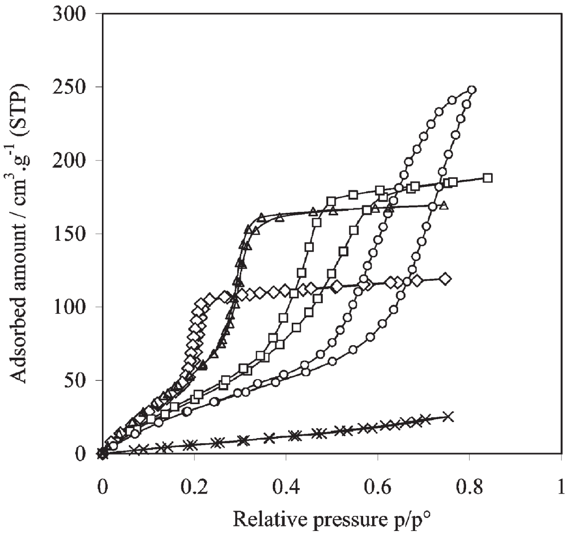

Fig. 1 Adsorption isotherms of hexane at 303 K over micelle-templated silicas of different pore sizes: (◇) 3.1 nm MCM-41, (△) 3.8 nm MCM-41, (□) 5.6 nm MCM-41, (○) 9.9 nm MCM-41 and (×) Aerosil 200.

The specific area can be derived from the BET transformation provided that the molecular diameter of the probe adsorbed can be determined, but more interestingly in our case, C_{BET} parameters can also be derived from this equation and are proportional to the adsorptive–adsorbent interaction. C_{BET} parameters can be defined according to:

$$C_{BET} = \exp\left(\frac{E_1 - E_l}{RT}\right) \qquad (3)$$

In mesoporous materials, the adsorption of nitrogen would yield C_{BET} values in the range of 60–100 but this range is only appropriate for nitrogen used as a probe and the comparison between C_{BET} obtained with different adsorbing probes is thus not straightforward. Indeed, when adsorbing other probe molecules, this range may shift either upwards or downwards, depending on the affinity of the adsorptive for the surface on which adsorption takes place.

Examples of BET transformations are shown in Fig. 2 in the case of the 3.1 nm and 9.9 nm MCM-41 materials. The curves obtained are almost straight lines in different pressure ranges, depending on the onset of capillary condensation from which the BET transform does not apply. These straight lines indicate that the BET model can be applied in the respective relative pressure ranges.

The results reported in Table 2 indicate that the monolayer coverages and the pore volumes evaluated by hexane adsorption are well correlated with the results from N_2 adsorption (Table 1). C_{BET} values are dramatically low, lower than 5, confirming the very poor affinity of hexane for siliceous surfaces. The implications of this particular point will be further discussed later.

The adsorption isotherms can also be compared with a reference isotherm obtained from the adsorption of hexane on a non-porous silica, in this case, Aerosil 200. The *t*-plots obtained for the 3.1 nm MCM-41 and the 5.6 nm MCM-41 are reported in Fig. 3. Fig. 3 is representative of all *t*-plots obtained in this work and identical features can be discussed. *t*-plots were first made for the evaluation of the microporosity estimated from the intercept between the straight line obtained at low thickness and the *y* axis. When the intercept is zero, which is the case for all the samples studied here, it can be concluded that the samples of interest are essentially non-microporous. Furthermore, the position of the positive deviation in the comparison plots with Aerosil allows one to determine the extent of surface at which pore filling begins. These data are reported in Table 2 as well as the data obtained from the BET transformation and the total pore volume estimated from the knees of the adsorption isotherms, when available.

It can be observed that, in the case of the smallest mesopores, the onset of pore filling occurs when the monolayer on the silica surface has not yet been completed. This superposition of phenomena can be expected to affect the adsorption mechanism for all samples except the one with the largest pores, 9.9 nm MCM-41, for which monolayer adsorption

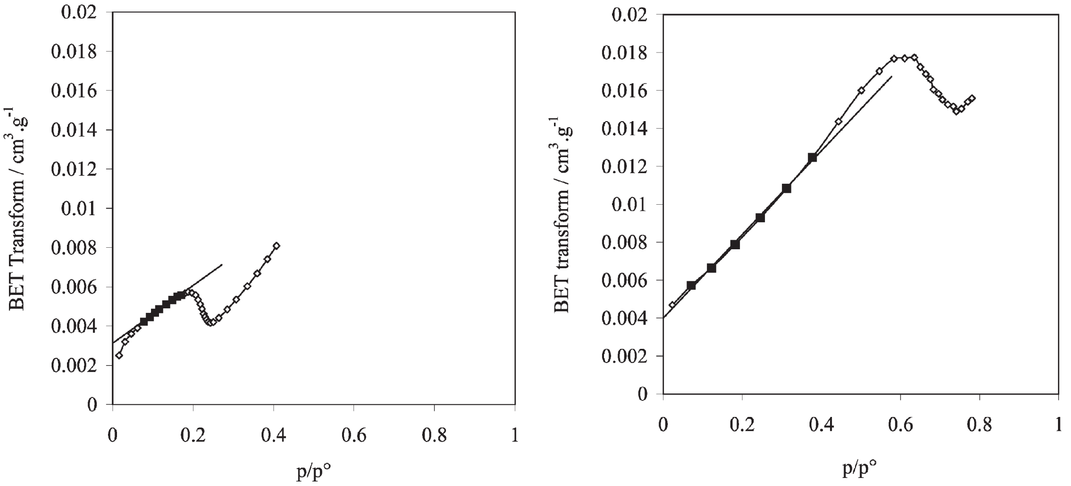

Fig. 2 BET transform of the adsorption isotherm of hexane at 303 K over the (left) 3.1 nm MCM-41 and (right) 9.9 nm MCM-41 materials.

and pore filling can be distinctly separated and proceed as usually expected, that is monolayer/multilayer adsorption mechanism *before* capillary condensation.

All C_{BET} values are very similar and do not depend on the pore width, which is not the case when adsorbing nitrogen over the same materials. We already mentioned that in the case of nitrogen adsorption over mesoporous materials, C_{BET} lies in the range 60–100 and become lower for larger pores and higher for smaller pores. This phenomenon is mainly due to dipole-quadrupole interactions between surface silanol groups and nitrogen molecules, so that as the pore size decreases the pore wall can more strongly interact with adsorbed molecules on the opposite surface of the pore. However, in the case presented here, hexane properties are mainly governed by dispersive forces, the strength of which, at long distances, is too weak to interact across the pore diameter between adsorbed molecules and the opposite surface of the pore.[21] As a conclusion, the C_{BET} values remain both very low and constant irrespective of the pore diameter.

From adsorption isotherms at several temperature levels, the classical isosteric heat of adsorption can be derived, provided both gas phase and adsorbed phase chemical potentials are identical. After intense discussions over a few decades,[15,22–26] it is usually admitted that this requirement is met on the desorption branch of sorption isotherms and this requirement is only appropriate in the case where adsorption and desorption paths are not superimposed.

At a given coverage, the differential isosteric enthalpy of sorption can be easily derived from an expression analogous to the Clausius–Clapeyron equation:

$$\left(\frac{\partial \ln p}{\partial T}\right)_{\Gamma} = -\frac{\Delta_{ads}\dot{h}}{RT^2} \qquad (4)$$

where p is the absolute equilibrium pressure at a given adsorbed amount Γ, R is the gas constant and T is the temperature at which the adsorption isotherm is determined.

Table 2 Adsorption of *n*-hexane at 303 K. Monolayer volume and *C* parameter from the BET equation, adsorbed amounts at the onset and completion of pore filling by comparison plot

Sample	N_m/ mmol g^{-1}	C_{BET}	N_{onset}/ mmol g^{-1}	N_p/ mmol g^{-1}
3.1 nm MCM-41	3.1	4.3	1.8	4.6
3.8 nm MCM-41	4.1	4.0	2.7	7.4
5.6 nm MCM-41	2.5	4.0	2.2	7.5
9.9 nm MCM-41	1.7	4.8	2.8	–

After integration, it yields:

$$(\ln p)_{\Gamma} = \frac{\Delta_{ads}\dot{h}}{RT} + \text{constant} \qquad (5)$$

In this way, the slope of a $(\ln p)_{\Gamma}$ *versus* $1/T$ plot provides a reliable evaluation of the differential enthalpy of adsorption, at least for coverage higher than about half a monolayer.[4] Moreover, the differential entropy of adsorption can also be readily calculated from the differential enthalpy of adsorption since at the equilibrium, $\Delta G_{adsorption} = 0$ kJ mol^{-1}. In this paper, comparison of the isotherms at the same fraction of pore filling has been used to calculate the differential enthalpy of adsorption (Fig. 4). These have been derived from both branches of the sorption isotherms and were found to be 1 kJ mol^{-1} apart for adsorption isotherms with hysteresis, which is in the range of the uncertainties given by microcalorimetric measurements. In Fig. 4, the adsorption enthalpy has been plotted as a function of the fraction of pore filling for all the adsorbents examined. Data can be found at fractions higher than unity since where the pore filling is complete (at the knees of the adsorption isotherms), there is still some adsorption on the external surface of the samples. The first point that can be made is that all enthalpy curves lie above the condensation enthalpy of hexane in the bulk (−31.8 kJ mol^{-1}). Furthermore, common trends can be observed for all enthalpy curves, trends that are consistent with classical adsorption processes: the adsorption heat (a) steadily decreases in the low coverage part of the curve, in which a monolayer is being formed on the overall surface of the adsorbent; (b) remains at a virtually constant value during the pore filling; (c) decreases towards the condensation enthalpy when pore filling has been completed and residual adsorption only takes place on the outer surface of the adsorbent. However, the curves differ in the absolute values of enthalpy and in the transition between monolayer formation and pore filling.

The pore filling enthalpy of hexane over 3.1 nm MCM-41 is in good agreement with published calorimetric data,[14,19] as well as the steady decrease of the pore filling enthalpy when pore size increases.[17b] In any case, the pore filling enthalpy is always higher than the condensation enthalpy, even in the case of 9.9 nm MCM-41. This result (also evidenced by Neimark *et al.*[15b] at low temperature using nitrogen and argon as probes) is apparently in contrast with accepted views on mesopore condensation. Furthermore, the enthalpic advantage of confinement seems to be inversely proportional to the pore size and has consequences to be evaluated on accepted models of capillary condensation. The Lennard-Jones kinetic diameter of *n*-hexane being 0.43 nm, the liquid phase is significantly stabilised in cavities as large as 23 molecular diameters.

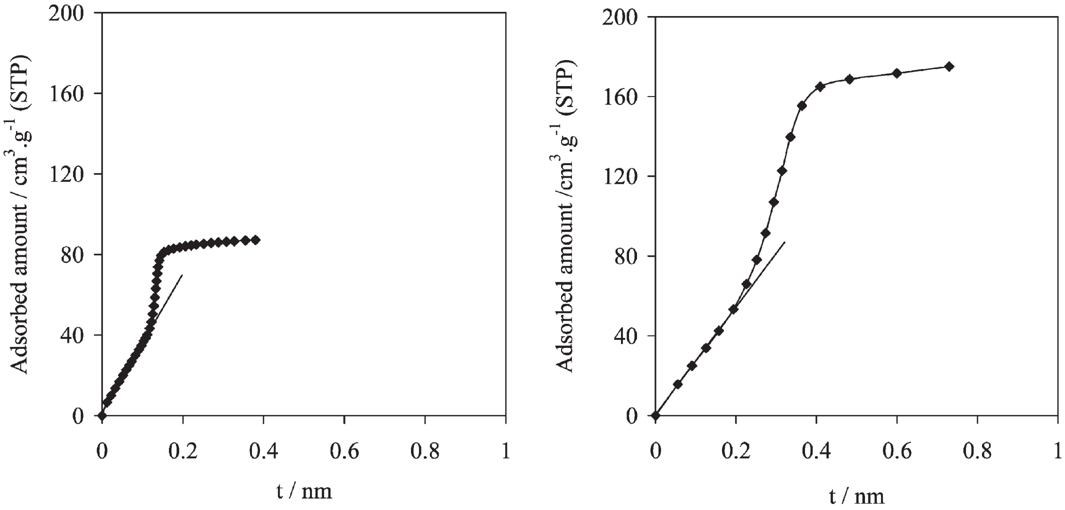

Fig. 3 *t*-plot traced from the adsorption isotherm of hexane over the (left) 3.1 nm MCM-41 and (right) 9.9 nm MCM-41 materials at 303 K, taking Aerosil 200 as a reference.

An even more important effect is that the nucleation of a liquid phase is more favoured than the completion of a monolayer for pores as large as up to 13 molecular diameters. Results in Fig. 4 also show that, in the case of the largest pore adsorbent, 9.9 nm MCM-41, monolayer formation and pore filling are well separated phenomena, separated by an intermediate adsorption at enthalpic values strictly corresponding to the bulk condensation enthalpy. This is confirmation of the very weak adsorptive–adsorbent interaction, even for the first adsorbed monolayer. This intermediate adsorption can be classically attributed to a multilayer adsorption, taking place on the pore surface before the onset of pore condensation.

It is especially interesting to observe that the adsorption enthalpy increases when pore condensation commences, keeping in mind that interactions from the pore walls cannot account for a large enthalpic excess of the hexane phase condensing in the core of the pores. This minimum in adsorption enthalpy can also be observed in the case of the adsorbents with smaller mesopores, but this trend is to some extent hidden by the superposition of the pore filling process and monolayer formation.

Discussion

Does this enthalpic effect need to be explained by a special state of the confined fluid in the mesopores or can it be justified by a mere effect of scale? Scale effects are usually described on the basis of the surface/volume ratio of the adsorbed phase. In the case of condensation in a mesopore, the volume of the adsorbed phase in the pores is well defined by the amount of adsorbate corresponding to the step of the type IV isotherm. The surface of the adsorbed phase corresponds to the interface between the layer adsorbed on the pore walls and the vapour phase at the onset of condensation. A cross-sectional view of a pore being filled by capillary condensation has been drawn in Fig. 5. The pore itself is defined by its diameter D_{pore} and its inner surface S_{pore}. The adsorbed phase defines both D_{filling} and $S_{\text{interface}}$, yielding the volume of the adsorbed phase, V_{filling}.

If the fluid in a filled mesopore is assumed to share the properties of the bulk liquid (especially the same density), the energetics of pore filling can be written as:

$$\Delta H_{\text{filling}} = \Delta H_{\text{condensation}} - N_{\text{interface}} \times \Delta h_{\text{interface}} \quad (6)$$

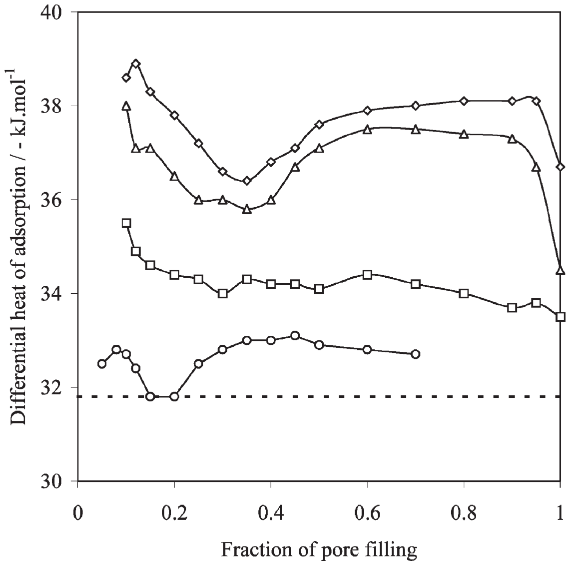

Fig. 4 Heat of adsorption of hexane as a function of coverage on: (◇) 3.1 nm MCM-41, (△) 3.8 nm MCM-41, (□) 5.6 nm MCM-41, (○) 9.9 nm MCM-41. Dashed line: condensation heat of hexane.

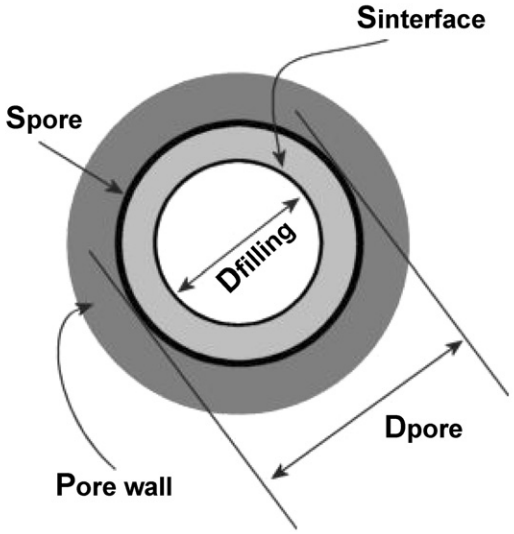

Fig. 5 Schematic representation of an adsorbed phase in a cylindrical mesopore.

Table 3 Comparison between calorimetric data obtained either from the isosteric method or calculated according to eqn. (11)

	V_{filling}/ cm^3 g^{-1}	V_{pore}/ cm^3 g^{-1}	$N_{\text{monolayer}}$/ mmol g^{-1}	$N_{\text{interface}}$/ mmol g^{-1}	Calcd $-h_{\text{filling}}$/ kJ mol^{-1}	Isosteric $-h_{\text{filling}}$/ kJ mol^{-1}
3.1 nm MCM-41	57	105	3.1	2.3	39.2	38.1
3.8 nm MCM-41	100	177	4.1	3.1	37.3	37.4
5.6 nm MCM-41	110	180	2.5	2.0	35.0	34.2
9.9 nm MCM-41	210	290	1.7	1.4	33.0	33.0

and for a mole of adsorptive:

$$\Delta h_{\text{filling}} = \Delta h_{\text{condensation}} - \frac{N_{\text{interface}}}{N_{\text{filling}}} \times \Delta h_{\text{interface}} \qquad (7)$$

This is to say that the molar enthalpy of pore filling is equal to the molar enthalpy of bulk condensation plus a contribution corresponding to the disappearance of the interface between adsorbed layer and vapour phase. This interface excess contribution is proportional to the interface fraction of adsorbate molecules and is the molar equivalent of a surface tension. In the case of a cylindrical pore, the fraction of molecules at the interface can be easily calculated under the simplifying assumption of constant density of the adsorbate.

Assuming that the surface of the first adsorbed monolayer corresponds to the surface of an empty pore (*i.e.*, $S_{\text{monolayer}} = S_{\text{pore}}$, which is realistic for mesopores), we obtain:

$$N_{\text{interface}}/N_{\text{monolayer}} = S_{\text{interface}}/S_{\text{monolayer}} \qquad (8)$$

where $N_{\text{interface}}$ corresponds to the number of molecules at the gas–adsorbed phase interface and $S_{\text{interface}}$ is the corresponding surface.

If V is defined as the pore volume, D_{pore} as the pore diameter, and l as the pore length, we have:

$$V = \pi \times D_{\text{pore}}^2 \times l/4 \text{ and } S = \pi \times D_{\text{pore}} \times l.$$

so that:

$$S_{\text{interface}}/S_{\text{monolayer}} = (V_{\text{filling}}/V_{\text{pore}})^{1/2} \qquad (9)$$

and therefore:

$$N_{\text{interface}} = N_{\text{monolayer}} \times \sqrt{\frac{V_{\text{filling}}}{V_{\text{pore}}}} \qquad (10)$$

Finally, from eqns. (7) and (10), this yields:

$$\Delta h_{\text{filling}} = \Delta h_{\text{condensation}} - \frac{N_{\text{monolayer}} \times \Delta h_{\text{interface}}}{N_{\text{filling}}} \times \sqrt{\frac{V_{\text{filling}}}{V_{\text{pore}}}} \qquad (11)$$

The adsorbed amount in the monolayer is accessible through the BET equation. The filling volume can be measured from the step corresponding to the mesopore filling on the sorption curve and the total adsorbed volume corresponds to the saturation plateau of the sorption isotherm. The molar interface enthalpy used in the calculations (8.1 kJ mol^{-1}) has been derived from the surface tension of *n*-hexane (0.018 N m^{-1}) by assuming an interface density equal to the density of an *n*-hexane monolayer on Aerosil 200 (2.21 μmol m^{-2}, readily derived from Fig. 1). The molar condensation enthalpy of bulk *n*-hexane has been taken as −31.8 kJ mol^{-1}.[27]

Isosteric differential enthalpies of pore filling have been evaluated for the adsorption of *n*-hexane in mesoporous silicas of several pore sizes and compared with calculated values. The results are reported in Table 3. The excellent agreement between calculated and experimental values vindicates the assumption of constant surface tension as the basis of the application of the Kelvin equation to the pores in the mesopore range. A variation of 1 kJ mol^{-1} between calculated and experimental data corresponds to the sensitivity threshold of the isosteric method and also suggests that the Tolman curvature effect on the surface tension is not higher than 15% for pores with diameters between 3 and 4 nm.[2]

The disappearance of the interface between vapour and adsorbed layer provides a rationale for the huge effect of the scale of the adsorbent on the energetics of adsorption for pores much larger than the upper limits of micropores.

Conclusion

Pore size effects, often reported in the literature but generally poorly explained, can be understood as a contribution from the surface tension, which has to be taken into account in the evaluation of the energetics of adsorption. The adsorption of hexane on mesoporous MCM-41 materials having different pore sizes has been studied and interesting behaviours have been found using the BET model and by tracing comparison plots.

A correlation between the heat of condensation and the pore size has been clearly established and this effect cannot be due to pore wall interactions. On the other hand, the enthalpic contribution of the liquid–gas interface to the overall process has been derived and precisely matches the difference between the enthalpy of condensation in the bulk and the enthalpy condensation in mesopores as large as 10 nm. This interfacial effect could shed new light on the thermodynamics of adsorption in small mesopores. More convincing proof of this effect could be given using either small mesopore materials (between 2 and 3 nm) or very large pore materials (beyond 10 nm). These two ranges of materials are not easy to prepare, mainly because keeping the honeycomb structure of the pores as ideal as possible is difficult. Nevertheless, additional studies are already under way. Further experiments are also currently being carried out by liquid-flow microcalorimetry, which will be exploited to extend these findings to other systems useful for separation technology and chromatography.

References

1 S. J. Gregg and K. S. W. Sing, *Adsorption, Surface Area and Porosity*, Academic Press, London, 2nd edn., 1982, p. 154.
2 R. C. Tolman, *J. Chem. Phys.*, 1949, **17**, 333.
3 W. S. Ahn, M. S. Jhon, H. Park and S. Chang, *J. Colloid Interface Sci.*, 1972, **38**, 605.
4 F. Rouquerol, J. Rouquerol and K. Sing, in *Adsorption by Powders and Porous Ssolids*, Academic Press, San Diego, 1999, p. 203.
5 J. S. Beck, J. C. Vartuli, W. J. Roth, M. E. Leonowicz, C. T. Kresge, K. D. Schmitt, C. T. W. Chu, D. H. Olson, E. W. Sheppard, S. B. McCullen, J. B. Higgins and J. L. Schlenker, *J. Am. Chem. Soc.*, 1992, **114**, 10834.
6 (*a*) O. Franke, G. Schulz-Ekloff, J. Rathousky, J. Starek and A. Zukal, *J. Chem. Soc., Chem. Commun.*, 1993, 724; (*b*) P. J. Branton, P. G. Hall, K. S. W. Sing, H. Reichert, F. Schüth and K. K. Unger, *J. Chem. Soc., Faraday Trans.*, 1994, **90**, 2965; (*c*) S. Z. Qiao, S. K. Bhatia and D. Nicholson, *Langmuir*, 2004, **20**, 389.
7 (*a*) P. I. Ravikovitch, S. C. O. Domhnaill, A. V. Neimark, F. Schüth and K. K. Unger, *Langmuir*, 1995, **11**, 4765; (*b*) K. Morishige and M. Shikimi, *J. Chem. Phys.*, 1998, **108**, 7821.

8 J. Rathousky, A. Zukal, O. Franke and G. Schulz-Ekloff, *J. Chem. Soc., Faraday Trans.*, 1995, **91**, 937.

9 M. Grün, K. K. Unger, A. Matsumoto and K. Tsutsumi, in *Characterisation of Porous Solids IV*, eds. B. McEnaney, T. J. Mays, J. Rouquérol, F. Rodrigruez-Reinoso, K. S. W. Sing and K. K. Unger, Royal Society of Chemistry, London, 1997, ch. 213, pp. 81–89.

10 J. Y. Ying, C. P. Mehnert and M. S. Wong, *Angew. Chem., Int. Ed.*, 1999, **38**, 56.

11 A. Sayari, Y. Yang, M. Kruk and M. Jaroniec, *J. Phys. Chem. B*, 1999, **103**, 3651.

12 K. Hanna, I. Beurroies, R. Denoyel, D. Desplantier-Giscard, A. Galarneau and F. Di Renzo, *J. Colloid Interface Science*, 2002, **252**, 101.

13 U. Ciesla, M. Grün, T. Isajeva, A. A. Kurganov, A. V. Neimark, P. Ravikovitch, S. Schacht, F. Schüth and K. K. Unger, in *Access in Nanoporous Materials*, eds. T. J. Pinnavaia and M. F. Thorpe, Plenum Press, New York, 1995, p. 231.

14 A. Galarneau, D. Desplantier, R. Dutartre and F. Di Renzo, *Microporous Mesoporous Mater.*, 1999, **27**, 297.

15 (*a*) C. Latoskie, K. E. Gubbins and N. Quirke, *J. Phys Chem.*, 1993, **97**, 4783; (*b*) A. Neimark, P. I. Ravikovitch, M. Grün, F. Schüth and K. K. Unger, *J. Colloid Interface Sci.*, 1998, **207**, 159.

16 M. Kruk and M. Jaroniec, *J. Phys. Chem. B*, 2002, **106**, 4732.

17 (*a*) J. C. P. Broekhoff and J. H. de Boer, *J. Catal.*, 1967, **9**, 8; (*b*) J. C. P. Broekhoff and J. H. de Boer, *J. Catal*, 1967, **9**, 15.

18 N. Tanchoux, P. Trens, D. Maldonado, F. Di Renzo and F. Fajula, *Colloids Surf.*, accepted.

19 J. Jnchen, H. Stach, M. Busio and J. H. M. C. Van Wolput, *Thermochim. Acta*, 1998, **312**, 33.

20 J. Israelachvili, *Intermolecular and Surface Forces*, Academic Press, London, 2nd edn., 1991, ch. 6.

21 D. H. Everett and J. C. Powl, *J. Chem. Soc., Faraday Trans. 1*, 1976, **72**, 619.

22 S. Brunauer, in *The Adsorption of Gases and Vapours*, Oxford University Press, London, 1945, p. 126.

23 D. H. Everett and J. M. Haynes, *Z. Phys. Chem.*, 1975, **97**, 301.

24 W. F. Saam and M. W. Cole, *Phys. Rev.*, 1975, **11**, 1086.

25 R. Evans, U. M. B. Marconi and P. Tarazona, *J. Phys. Chem.*, 1986, **84**, 2376.

26 C. G. V. Burgess, D. H. Everett and S. Nutall, *Pure Appl. Chem.*, 1989, **61**, 1845.

27 R. C. Reid, J. M. Prausnitz and T. K. Sherwood, *The Properties of Gases and Liquids*, McGraw-Hill, New York, 1977.